a "hydrothermal NMR tube"[20] is used instead. The reference $\delta = 0$ was to an external aqueous solution of $Al(NO_3)_3$ (1M).

X-ray crystal structure analysis: A crystal fragment was placed into a capillary Lindemann glass to prevent dehydratation. Intensities were recorded on a Bruker SMART CCD diffractometer ($Mo_{K\alpha}$ radiation $\lambda =$ 0.71073 Å, graphite monochromator) at 300 K. An empirical absorption correction was applied using the SADABS program.[21] 45869 unique reflections ($R_{int} = 0.0746$) were used ($1.31^\circ < \theta < 29.83^\circ$). The structure was solved and refined using the program package SHELXTL 5.03.[22] The examination of the systematic absences is consistent with the space groups *C*2/*c* (No. 15) or *Cc* (No. 9). The structure was first solved in the space group *C*2/*c*. Five sulfate groups were located from the observating successive Fourier map analyses. One SO_4^{2-} ion is placed nearby on the *2* axis (at 0, *y*, ¼), which induces a short S–S distance of 1.45 Å. A statistical disorder must occur for this SO_4^{2-} ion and the occupancy factor was refined to 50%; it corresponds to 4.5 SO_4^{2-} ions for 15 Al atoms (or nine SO_4^{2-} ions per Al_{30}). At this stage, some SO_4^{2-} groups were refined with geometrical restraints and water molecules were located approximately due to their very diffuse average electronic density. The sulfate counterions may not all be accurately positioned. With such a strategy the structure can be described as follows: $Al_{30}O_8(OH)_{56}(H_2O)_{24}(SO_4)_9 \cdot x\,H_2O$ ($x > 35$), monoclinic, space group *Cc* (No. 9), $a = 28.0259(5)$, $b = 19.4890(3)$, $c =$ 28.9883(5) Å, $\beta = 112.514(1)^\circ$, $V = 14626.6(4)$ Å^3, $Z = 4$, $\rho_{calc} =$ 1.588 g cm^{-3}, $\mu = 0.452$ mm^{-1}, crystal size $0.38 \times 0.26 \times 0.12$ mm^3. Crystallographic data (excluding structure factors) for the structure reported in this paper have been deposited with the Fachinformationszentrum Karlsruhe. Further details may be obtained from FIZ, 76344 Eggenstein-Leopoldshafen, Germany (fax: (+49) 7247-808-666; e-mail: crysdata @fiz-karlsruhe.de) on quoting the depository number CSD-410995.

Received: October 7, 1999 [Z14125]

[1] a) J. W. Akitt, J. M. Elders, X. L. R. Fontaine, A. K. Kundu, *J. Chem. Soc. Dalton Trans.* **1989**, 1889–1895; b) J. W. Akitt, J. M. Elders, X. L. R. Fontaine, A. K. Kundu, *J. Chem. Soc. Dalton Trans.* **1989**, 1897–1901.

[2] J. P. Jolivet in *De la Solution à l'Oxyde (*Eds.: M. Henry, J. Livage*)*, CNRS, Paris, **1994**.

[3] J. Y. Bottero, D. Tchoubar, J. M. Cases, F. Flessinger, *J. Phys. Chem.* **1982**, *86*, 3667–3673.

[4] a) D. R. Parker, P. M. Bertsch, *Environ. Sci. Technol.* **1992**, *26*, 908–914; b) D. R. Parker, P. M. Bertsch, *Environ. Sci. Technol.* **1992**, *26*, 914–921.

[5] P. H. Hsu, *Clays Clay Miner.* **1997**, *45*, 286–289.

[6] R. C. Turner, *Can. J. Chem.* **1976**, *54*, 1910–1915.

[7] a) J. T. Kloprogge, D. Seykens, J. W. Geus, J. B. H. Jansen, *J. Non-Cryst. Solids* **1992**, *142*, 87–93; b) J. T. Kloprogge, D. Seykens, J. W. Geus, J. B. H. Jansen, *J. Non-Cryst. Solids* **1992**, *142*, 94–102.

[8] L. F. Nazar, G. Fu, A. D. Bain, *Chem. Mater.* **1991**, *3*, 602–610.

[9] G. Johansson, *Acta Chem. Scand.* **1960**, *14*, 771–773.

[10] G. Johansson, G. Lundgren, L. G. Sillen, R. Söderquist, *Acta Chem. Scand.* **1960**, *14*, 769–771.

[11] A. Müller, S. Q. N. Shah, H. Bogge, M. Schmidtmann, *Nature* **1999**, *397*, 48–50.

[12] L. C. W. Baker, J. S. Figgis, *J. Am. Chem. Soc.* **1970**, *92*, 3794–3797.

[13] M. T. Pope, A. Müller in *Polyoxometalates: From Platonic Solids to Anti-Retroviral Activity,* Kluwer Academic, Dordrecht, **1994**.

[14] C. L. Hill, *Chem. Rev.* **1998**, *98*, 1–390.

[15] K. Wassermann, R. Knut, H. J. Lunk, J. Fuchs, N. Steinfeld, R. Stösser, *Inorg. Chem.* **1995**, *34*, 5029–5036.

[16] L. Z. Pauling, *Kristallokhim. Miner.* **1933**, *84*, 442.

[17] W. O'Neil Parker, R. Millini, I. Kiricsi, *Inorg. Chem.* **1997**, *36*, 571–575.

[18] G. Turco, PhD thesis, Université de Nice (France), **1962**.

[19] A. C. Kunwar, A. R. Thompson, H. S. Gutowsky, E. Oldfield, *J. Magn. Reson.* **1984**, *60*, 467–472.

[20] C. Gerardin, M. In, F. Taulelle, *J. Chim. Phys. Phys. Chim. Biol.* **1995**, *92*, 1877.

[21] G. M. Sheldrick, SADABS (the Siemens Area Detector ABSorption correction), University of Göttingen, **1996**.

[22] G. M. Sheldrick, SHELXTL 5.03, Bruker Analytical X-ray Systems, Madison, WI, **1994**.

[23] During submission of this contribution L. F. Nazar, Waterloo University, Canada mentioned her findings of an isolated Al_{13} δ-Keggin isomer and of an Al_{30} cluster.

The Vibrational Inelastic Neutron Scattering Spectrum of Dodecahedrane: Experiment and DFT Simulation**

Bruce S. Hudson,* Dale A. Braden, Stewart F. Parker, and Horst Prinzbach

Because of its high symmetry (I_h) the hydrocarbon dodecahedrane ($C_{20}H_{20}$)[1–4] provides a classic case for vibrational analysis and, as a result, a rigorous test of the methods of ab initio or density functional normal-mode analysis. Under the I_h point group the 114 normal modes of vibration are classified into $2A_g + 1T_{1g} + 2T_{2g} + 4G_g + 6H_g + 3T_{1u} + 4T_{2u} + 4G_u + 4H_u$ symmetry types. There are only 30 discrete vibrational frequencies due to the high average degeneracy. Of these only the $3T_{1u}$ modes are active in the IR spectrum and only the $2A_g$ and $6H_g$ modes are active in the Raman spectrum. Thus 19 of the 30 modes of vibration are unobservable by these optical methods so long as this molecule retains its high symmetry.

Inelastic neutron scattering (INS) spectroscopy is not subject to the restrictions of optical selection rules. This permits all modes to be observed in proportion to the extent to which hydrogen-atom motions contribute to that mode. From a set of calculated normal-mode eigenvectors and

[*] Prof. B. S. Hudson
Department of Chemistry, Syracuse University
Syracuse, NY 13244-4100 (USA)
Fax: (+1) 315-443-4070
E-mail: bshudson@syr.edu

D. A. Braden
Department of Chemistry, University of Oregon
Eugene, OR 97403 (USA)

Dr. S. F. Parker
ISIS Facility, Rutherford Appleton Laboratory
Chilton, Didcot OX 11 0QX (UK)

Prof. H. Prinzbach
Chemisches Laboratorium der Universität
Institut fur Organische Chemie und Biochemie
79104 Freiburg (Germany)

[**] The Rutherford Appleton Laboratory is thanked for access to neutron beam facilities at ISIS. This work was partially supported by the US National Science Foundation (grant CHE 9803058) and utilized the computer systems Exemplar and SGI PCarray at the National Center for Supercomputing Applications, University of Illinois at Urbana-Champaign. We thank Chris Middleton of Syracuse University for development of the program used to plot neutron spectra.

  0570-0833/00/3903-0514 $ 17.50+.50/0

eigenvalues, it is a straightforward matter to calculate the neutron scattering vibrational intensities for a hydrogen-containing species for direct comparison with experiment. This reduces the ambiguity in spectral assignment and provides an additional comparison between the results of calculation and experiment. Recent advances in density functional theory (DFT) for large molecules permit reliable normal-mode calculations. Recent progress in the methods of inelastic neutron scattering spectroscopy allow use of relatively small samples and provide improved resolution. Here we show how these developments fit together. Dodecahedrane is a particularly nice case for a neutron scattering study because its large mass combined with its high symmetry results in a well-resolved spectrum.

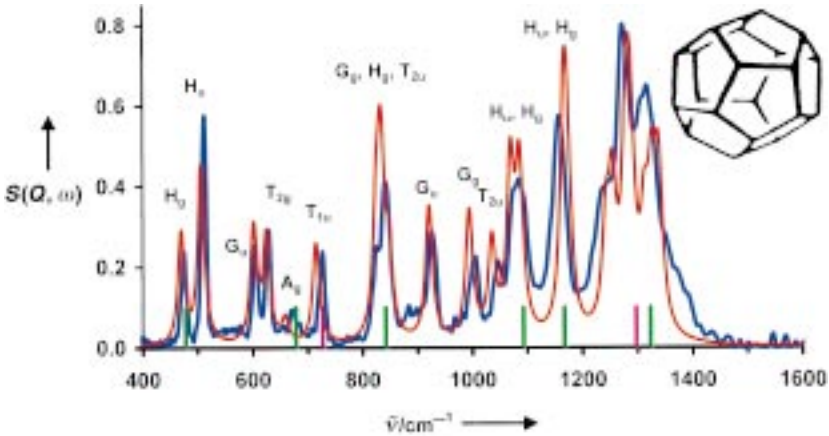

Figure 1. The inelastic neutron scattering spectrum of dodecahedrane (obtained at ISIS with TOSCA, see the Experimental Section). The sample is at a temperature of 15 K. The experimental spectrum is shown in blue. The results of the DFT calculation are shown in red (the calculated frequencies have been multiplied by a factor of 0.99 to improve agreement with experiment). The vertical green lines indicate the reported positions of the Raman-active H_g and A_g transitions, and the vertical pink lines indicate the reported positions of the IR-active T_{1u} transitions (see Table 1).[3–5] The symmetry labels are from the DFT calculation.

The major results of this study are presented in Table 1 and Figure 1 (a broad, complex phonon peak centered at 50 cm^{-1} and extending from 25 to 75 cm^{-1} is not shown). The first point to note is that all of the optical (mostly Raman) frequencies are in good agreement with observed neutron scattering features. This permits identification of these features as due to A_g or H_g (or T_{1u}) symmetry modes. Many other strong features not seen in the optical spectra are observed as expected, illustrating the utility of inelastic neutron scattering.

The degree of agreement between the calculated and observed spectra provides confidence that at least in the frequency region shown the observed transitions can be identified with certainty. Some of the bands at higher frequency are composite and await improvements in resolution for their separation. In all cases the calculation produces features with the correct symmetry to account for the Raman and IR features. In the region below 1200 cm^{-1} the features are mostly distinct except for the overlapping bands near 850 cm^{-1} and the two pairs at 1100 and 1180 cm^{-1}. All vibrations give rise to observed features (subject to overlap)—there are no "silent" modes in the INS spectrum. The origin of the activity of these skeletal modes with a technique that depends on the motion of hydrogen atoms is that the rigid attachment of the hydrogen atoms to their respective carbon atoms causes them to follow the carbon-atom motions.

Table 1. Vibrations of dodecahedrane.

Symmetry[a]	Calcd [cm^{-1}][b]	Reported [cm^{-1}]	INS [cm^{-1}][c]
H_g	481	479,[d] 480[e]	477
H_u	518		514
G_u	615		607
T_{2g}	639		632
A_g	673	679,[d] 676[e]	675
T_{1u}	731	728[f]	727
G_g	843		(845)
H_g	852	843,[d] 840[e]	(845)
T_{2u}	866		(845)
G_u	941		930
G_g	1016		1007
T_{2u}	1058		1050
H_u	1093		(1089)
H_g	1110	1094,[d] 1092[e]	(1089)
H_u	1192		(1164)
H_g	1198	1168,[d] 1164[e]	(1164)
T_{2u}	1269		1270 sh
G_g	1282		1282
T_{1g}	1305		
T_{2g}	1309		1310
H_u	1316		1320
T_{1u}	1341	1298[f]	
G_u	1354		1380 sh
H_g	1367	1324[e]	

[a] In point group I_h. [b] DFT/b3lyp/6-31G**. [c] Values from the inelastic neutron scattering spectrum. Numbers in parentheses indicate that all peaks so marked overlap nearby peaks. [d] Raman data from ref. [5]. [e] Raman data from refs. [3, 4]. [f] IR data from refs. [3 4].

The lowest wavenumber features observed at 477 and 514 cm^{-1} are the H_g and H_u transitions. The relatively high intensity of these signals may be ascribed to the fivefold degeneracy. The calculation predicts that these two transitions should have more equal intensities than is observed (see below).

No splitting is seen at this resolution for these or any other isolated transitions. The neutron spectrum is consistent with I_h symmetry.[6] The next four transitions are also resolved features with degeneracies of 4, 3, 1, and 3, respectively. These are followed by an overlapping triplet with the appropriate total intensity and then by three more isolated transitions with degeneracies of 4, 4, and 3, respectively. The intensities are roughly proportional to the degeneracies, but the calculations show that over this spectral region there is a variation in intrinsic intensity (i.e., a fractional contribution of hydrogen-atom motion to the total motion of a particular vibrational normal coordinate) by almost a factor of 2.

These individual transitions are followed by two pairs of H_u and H_g transitions. The H_g frequency is above that of the H_u values in each case, as indicated by the fact that the Raman-active H_g transition is seen on the high side of each of the composite neutron bands. This is consistent with the calculation. Also, the predicted H_u/H_g separations of 17 and 6 cm^{-1} appear to be appropriate to the observations.

  0570-0833/00/3903-0515 $ 17.50+.50/0

In the region from 1200 – 1400 cm^{-1} a total of eight transitions are expected with symmetries of T_{2u}, G_g, T_{1g}, T_{2g}, H_u, T_{1u}, G_u, H_g (in order of increasing frequency). This order is consistent with the observation of the H_g Raman band on the high-frequency side of the composite band and the appearance of the IR line due to the T_{1u} transition at a frequency lower than the Raman line. There are clearly additional transitions in the INS spectrum at frequencies lower than the observed IR line, also in agreement with the calculated state ordering.

This spectrum illustrates the power of INS in the determination of vibrational transitions that are forbidden by optical spectroscopies. The spectrum of dodecahedrane is notable for the absence of phonon side bands, which are usually increasingly important features at higher frequency. This is in contrast, for example, to the similar molecule adamantane,[7] where clear phonon wings are observed on all transitions. This difference is probably associated with the smaller amplitude of motion of each atom in the larger dodecahedrane species. The absence of phonon side bands greatly simplifies the interpretation of the spectrum.

This preliminary comparison also demonstrates the utility of INS spectroscopy as a method of testing ab initio/DFT or empirical normal-mode calculations, at least in so far as they provide an adequate description of the participation of hydrogen-atom motions in a normal mode of motion. The new frequencies provided can of course be used for direct comparison with frequencies calculated using other methods. In this way a previous empirical normal-mode calculation of dodecahedrane[8] is seen to be rather inaccurate. Simulations of the spectral intensity permit added confidence in spectral assignments, even when there is considerable overlap of transitions.

The major residual difference between the calculated and observed INS spectrum is the relative intensity between the first two peaks (H_g and H_u symmetry). Another point is that, in contrast to recent studies of the longitudinal acoustic modes of *n*-alkanes,[9] we find that for dodecahedrane a slight shift of the spectral scale is needed to match the spectral features. For the related molecule adamantane this effect is considerably larger than for dodecahedane. For the out-of-plane bending modes of the *n*-alkanes there is a considerable shift of the frequencies to higher values relative to those from DFT calculations that correctly predict the longitudinal acoustic modes.[9] It is clear in this last case that this is due to intermolecular interactions. It is suspected that intermolecular interactions are the origin of the small shift and intensity effects for dodecahedrane, but this conclusion is complicated by the observation that for adamantane an MP-2 calculation appears to provide much better agreement for frequencies than does the DFT result. This may be due to compensation of effects. More work is required to resolve these issues.

Experimental Section

Inelastic neutron scattering experiments were carried out at the ISIS spallation pulsed neutron source of the Rutherford Appleton Laboratory using the spectrometer TOSCA,[10] which had a current configuration of ten backscattering banks and was located at 12 m from the moderator. The resolution at this stage is about 2 % $\Delta E/E$ full width at half height through the energy range presented in this study. The synthesis and characterization of the dodecahedrane have been discussed.[1, 2] The sample was 260 mg of high-purity solid dodecahedrane in an aluminum foil sachet contained in an aluminum cell for protection. The cell was mounted in a cryostat held at 15 K. Data were collection for 20 h with ISIS operating at about 180 μA of proton current. The raw data was converted into the dimensionless $S(Q,\omega)$ using the standard analysis program GENIE. The spectral data were collected from 16 to 4000 cm^{-1}. The region above 1600 cm^{-1} was devoid of recognizable features (as expected) except for a broad CH stretch band.

The optimized geometry and normal modes of vibration of dodecahedrane were calculated using Gaussian 98.[11] The B3LYP density functional was used with a 6-31G** basis. The neutron scattering spectral calculations were performed by computing the sum of the squares of the amplitudes of the hydrogen-atom motion for each normal mode.[9, 12, 13] This is the amplitude of a Lorentzian peak at the normal-mode frequency for each vibration. The width of the Lorentzian lines was chosen to match the observed spectrum. This width is a linearly increasing function of frequency, as suggested by experimental design and calibration experiments.

Received: August 31, 1999 [Z13947]

[1] M. Bertau, F. Wahl, A. Weiler, K. Scheumann, J. Wörth, M. Keller, H. Prinzbach, *Tetrahedron* **1997**, *53*, 10029.

[2] M. Bertau, J. Leonhardt, A. Weiler, K. Weber, H. Prinzbach, *Chem. Eur. J.* **1996**, *2*, 570.

[3] L. A. Paquette, R. J. Ternansky, D. W. Balogh, G. Kentgen, *J. Am. Chem. Soc.* **1983**, *105*, 5446.

[4] R. J. Ternansky, D. W. Balogh, L. A. Paquette, *J. Am. Chem. Soc.* **1982**, *104*, 4503.

[5] S. H. Bertz, G. A. Kourouklis, A. Jayaraman, G. Lannoye, J. M. Cook, *Can. J. Chem.* **1993**, *71*, 352.

[6] The IR spectrum of this sample clearly indicates weak features at spectral positions that, on the basis of the neutron scattering and DFT results, we can identify as ungerade vibrations (T_{2u}, G_u, and H_u). This weak activity is consistent with the T_h site group symmetry reported for the crystal.[1] This spectrum and the corresponding lattice-induced Raman spectrum will be discussed in a later paper.

[7] http://www.isis.rl.ac.uk/insdata/.

[8] C. Coulombeau, A. Rassat, *J. Chim. Phys.* **1988**, *85*, 369.

[9] S. F. Parker, D. A. Braden, J. A. Tomkinson, B. S. Hudson, *J. Phys. Chem. B* **1998**, *102*, 5955; D. A. Braden, S. F. Parker, J. Tomkinson, B. S. Hudson, *J. Chem. Phys.* **1999**, *111*, 429.

[10] S. F. Parker, C. J. Carlile, T. Pike, J. Tomkinson, R. J. Newport, C. Andreani, F. P. Ricci, F. Sachetti, M. Zoppi, *Physica B* **1998**, *154*, 241 – 243.

[11] M. J. Frisch, G. W. Trucks, H. B. Schlegel, G. E. Scuseria, M. A. Robb, J. R. Cheeseman, V. G. Zakrzewski, J. A. Montgomery, Jr., R. E. Stratmann, J. C. Burant, S. Dapprich, J. M. Millam, A. D. Daniels, K. N. Kudin, M. C. Strain, O. Farkas, J. Tomasi, V. Barone, M. Cossi, R. Cammi, B. Mennucci, C. Pomelli, C. Adamo, S. Clifford, J. Ochterski, G. A. Petersson, P. Y. Ayala, Q. Cui, K. Morokuma, D. K. Malick, A. D. Rabuck, K. Raghavachari, J. B. Foresman, J. Cioslowski, J. V. Ortiz, B. B. Stefanov, G. Liu, A. Liashenko, P. Piskorz, I. Komaromi, R. Gomperts, R. L. Martin, D. J. Fox, T. Keith, M. A. Al-Laham, C. Y. Peng, A. Nanayakkara, C. Gonzalez, M. Challacombe, P. M. W. Gill, B. Johnson, W. Chen, M. W. Wong, J. L. Andres, C. Gonzalez, M. Head-Gordon, E. S. Replogle, J. A. Pople, *Gaussian 98*, Revision A.5, Gaussian, Inc., Pittsburgh PA, **1998**.

[12] B. S. Hudson, A. Warshel, R. G. Gordon, *J. Chem. Phys.* **1974**, *61*, 2929.

[13] A. C. Zemach, R. J. Glauber, *Phys. Rev.* **1956**, *101*, 118; A. C. Zemach, R. J. Glauber, *Phys. Rev.* **1956**, *101*, 129.

  0570-0833/00/3903-0516 $ 17.50+.50/0